

Multiple Quantum Oscillations in the de Haas–van Alphen Spectra of the Underdoped High-Temperature Superconductor $\text{YBa}_2\text{Cu}_3\text{O}_{6.5}$

Alain Audouard,¹ Cyril Jaudet,¹ David Vignolles,¹ Ruixing Liang,^{2,3} D. A. Bonn,^{2,3} W. N. Hardy,^{2,3} Louis Taillefer,^{3,4} and Cyril Proust^{1,3,*}

¹Laboratoire National des Champs Magnétiques Intenses (CNRS), Toulouse, France

²Department of Physics and Astronomy, University of British Columbia, Vancouver, Canada

³Canadian Institute for Advanced Research, Toronto, Canada

⁴Département de Physique & RQMP, Université de Sherbrooke, Sherbrooke, Canada

(Received 2 December 2008; published 6 October 2009)

By improving the experimental conditions and extensive data accumulation, we have achieved very high precision in the measurements of the de Haas–van Alphen effect in the underdoped high-temperature superconductor $\text{YBa}_2\text{Cu}_3\text{O}_{6.5}$. We find that the main oscillation, so far believed to be single frequency, is composed of three closely spaced frequencies. We attribute this to bilayer splitting and warping of a single quasi-2D Fermi surface, indicating that c axis coherence is restored at low temperature in underdoped cuprates. Our results do not support the existence of a larger frequency of the order of 1650 T reported recently in the same compound [S. E. Sebastian *et al.*, *Nature (London)* **454**, 200 (2008)].

DOI: 10.1103/PhysRevLett.103.157003

PACS numbers: 74.25.Ha, 74.25.Bt, 74.25.Jb, 74.72.Bk

The first unambiguous observation of quantum oscillations (QO) in high-temperature superconductors (HTSC) [1] has raised much interest concerning the origin of their Fermi surface (FS). On the overdoped side, recent quantum oscillations measurements in $\text{Tl}_2\text{Ba}_2\text{CuO}_{6+\delta}$ [2] (Tl-2201) have confirmed that the Fermi surface consists of a single large cylinder covering 65% of the first Brillouin zone (FBZ) as shown by angular magnetoresistance oscillations (AMRO) [3] or angle-resolved photoemission spectroscopy (ARPES) [4], in agreement with Hall effect data [5] and band structure calculations based on local-density approximation [6,7]. This result demonstrates that QO probe directly the FS originating from the CuO_2 planes and that the in-field QO agree with zero-field measurements.

On the underdoped side, both Shubnikov–de Haas [1,8,9] and de Haas–van Alphen (dHvA) [10,11] oscillations have been observed in underdoped $\text{YBa}_2\text{Cu}_3\text{O}_y$ (YBCO) pointing to a FS dramatically different from that of overdoped Tl-2201. Indeed, provided that quantum oscillations are interpreted as the consequence of quantization of closed orbits in a magnetic field [12], it can be inferred that the FS consists of small pockets covering only about 2% of the FBZ [1,8,9]. One fundamental question for our understanding of high-temperature superconductors is what causes the dramatic change in FS topology from overdoped to underdoped regimes [13–15]? Based on the observation of a negative Hall effect at low temperature in underdoped YBCO [16], the presence of an electron pocket in the Fermi surface has been suggested. It would naturally arise from a reconstruction of the large hole FS calculated from band structure. Different mechanisms have been proposed for this FS reconstruction, involving d -density-wave order (a scenario based on a hidden broken symmetry of $d_{x^2-y^2}$ type) [17], incommensurate antiferromagnetic order [11,18], stripe order [19], or field induced spin density

wave state [20,21]. Each scenario predicts a different FS topology, and the observation of an additional frequency would provide a stringent test. In particular, recent dHvA measurements [11] (performed in the same compound grown at the University of British Columbia as in Ref. [10] and the present study) seem to indicate the presence of a larger pocket, which would impose a strong constraint on the ordering wave vector for the reconstruction.

In order to determine whether there are other closed sections of the FS, something of fundamental importance for clarifying the FS of HTSC in the pseudogap phase, we have performed high-precision measurements of the de Haas–van Alphen effect in underdoped $\text{YBa}_2\text{Cu}_3\text{O}_y$ ($y = 6.51$ and $y = 6.54$). We found no evidence of an oscillatory component of high frequency as reported in Ref. [11], but the sensitivity of the measurements allows the uncovering of some important details for the electronic structure of underdoped YBCO. In addition to the main frequency $F_1 = 540$ T, two closely spaced satellites $F_2 = 450$ T and $F_3 = 630$ T have been resolved. We attribute these frequencies to a bilayer effect and warping of the FS, which proves that quasiparticle motion along the interplane direction is coherent at low temperature in the underdoped regime.

In order to achieve high-precision measurements of the de Haas–van Alphen effect, we have averaged several pulses (up to 10) for the same experimental conditions, as described in more detail in [10]. We have measured two single crystals: $\text{YBa}_2\text{Cu}_3\text{O}_{6.51}$ ($T_c = 57.5$ K) and $\text{YBa}_2\text{Cu}_3\text{O}_{6.54}$ ($T_c = 60$ K), flux grown in a nonreactive BaZrO_3 crucible. The dopant oxygen atoms were ordered into the ortho-II superstructure of alternating full and empty CuO chains [22]. Typical dimensions of the samples are $140 \times 140 \times 40 \mu\text{m}^3$. A careful study of the amplitude of the oscillations between the up- (50 ms) and down- (250 ms) field sweeps shows that the sample temperature

changes very little during the pulse. Given an effective mass of $m^* = 1.8m_0$ [10], the upper bound for the temperature difference is about 0.2 K at $T = 0.7$ K, which excludes any large heating effects during the pulse.

Figure 1 displays the field dependence of the oscillatory torque in two ortho-II samples, obtained after averaging up to 10 pulses during the down-field sweep at $T = 0.7 \pm 0.2$ K. A polynomial monotonic background has been subtracted from the raw data. While the amplitude of the oscillations should grow exponentially with magnetic field for a single frequency, a modulation of the amplitude of the oscillation (beating effect) can be noticed in both samples, which is the signature of the existence of more than one frequency in the oscillatory spectrum. Solid lines in Fig. 1 are fits of the Lifshitz-Kosevich (LK) theory, assuming that four frequencies are involved in the data, as discussed in more detail below.

In the framework of the LK theory, the field-dependent oscillatory part of the torque, for a multiband 2D Fermi surface, can be written: $\tau_{\text{osc}} = B \sum_i A_i \sin[2\pi(\frac{F_i}{B} - \gamma_i)]$, where F_i is the oscillation frequency linked to a given orbit and γ_i is a phase factor. Neglecting magnetic breakdown and spin damping contributions, the amplitude of a given Fourier component $A_i \propto R_{Ti} R_{Di}$, where $R_{Ti} = \alpha T m_i^* / B \sinh[\alpha T m_i^* / B]$ and $R_{Di} = \exp[-\alpha T_{Di} m_i^* / B]$ are the thermal and Dingle damping factors, respectively. Here, $\alpha = 2\pi^2 k_B m_0 / e\hbar = 14.69$ T/K and T_{Di} is the Dingle temperature [12]. In order to restrict the number of free parameters in the data analysis, we have considered the asymptotic form:

$$\tau_{\text{osc}} = \sum_i C_i \exp\left(-\frac{B_i}{B}\right) \sin\left[2\pi\left(\frac{F_i}{B} - \gamma_i\right)\right], \quad (1)$$

where $B_i = \alpha(T + T_{Di})m_i^*$. Strictly speaking, the latter assumption is only valid in the high T/B range and only

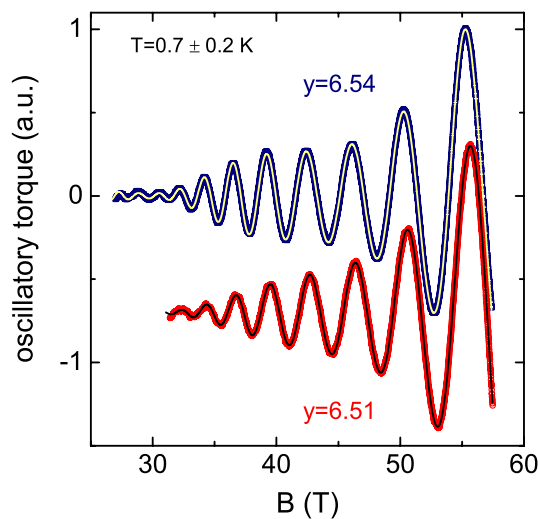


FIG. 1 (color online). Oscillatory part of the torque signal for underdoped $\text{YBa}_2\text{Cu}_3\text{O}_{6.54}$ (upper blue line) and $\text{YBa}_2\text{Cu}_3\text{O}_{6.51}$ (lower red line). Solid lines are best fits of Eq. (1) to the data. Four Fourier components are involved in the fit (see text).

affects the amplitude of the signal. The analysis is based on discrete Fourier transforms (DFT) using Blackman windows, which are known to avoid secondary lobes.

Figure 2(a) displays the field dependence of the oscillatory torque of $\text{YBa}_2\text{Cu}_3\text{O}_{6.54}$ (symbols). The solid line is a fit to the data assuming only one frequency $F_1 = 541$ T (solid line), which cannot match the dHvA data over a wide field range. This shows that the data *cannot* be accounted for by only one Fourier component. A large residual (i.e., the difference between the fit and the data) can be observed in Fig. 2(b) (symbols). The oscillatory spectrum still looks complicated, which means that more than one frequency is involved. DFT on this residual reveal the presence of two frequencies close to F_1 . The black line in Fig. 2(b) is a fit to the data with a second Fourier component $F_2 = 453$ T, whose residual is now displayed in Fig. 2(c) (symbols). The solid line in Fig. 2(c) is a fit with a third frequency $F_3 = 637$ T. Finally, the residual in Fig. 2(d) still contains a small component at $F_4 = 1119$ T, which we assume is the second harmonic of F_1 . The final residual is displayed in Fig. 2(e). The same kind of analysis performed on $\text{YBa}_2\text{Cu}_3\text{O}_{6.51}$ gives similar results. The averaged frequen-

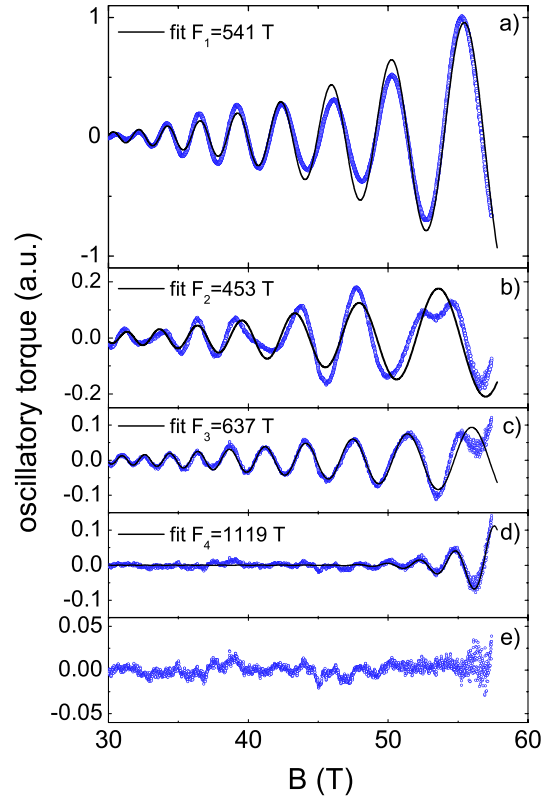


FIG. 2 (color online). (a) Oscillatory part of the torque signal for $\text{YBCO}_{6.54}$ (symbols). The black solid line is the best fit of Eq. (1) to the data with only the main frequency $F_1 = 541$ T. (b) Residual (fit data) of the previous fitting (symbols). The line shows the best fit of Eq. (1) to the data with two frequencies F_1 and $F_2 = 453$ T. The two other panels show the same procedure by taking into account (c) a third frequency $F_3 = 637$ T and (d) a fourth frequency $F_4 = 1119$ T. (e) Residual of the final fit.

cies deduced from the fits of Eq. (1) to the oscillatory torque of the two samples are $F_1 = 540 \pm 15$ T, $F_2 = 450 \pm 15$ T, $F_3 = 630 \pm 40$ T, and $F_4 = 1130 \pm 20$ T.

The corresponding Fourier analysis of the data for $\text{YBa}_2\text{Cu}_3\text{O}_{6.54}$ and $\text{YBa}_2\text{Cu}_3\text{O}_{6.51}$ are displayed in symbols in Figs. 3(a) and 3(b), respectively. A broad peak with a maximum around 535 T is observed, in agreement with [1,10]. The DFT of the fit involving only the F_1 component [large peak at 540 T (yellow online) in Fig. 3] cannot reproduce the tail and the small maxima on either side of the broad peak. These features are further evidence for the two additional frequencies F_2 [medium peak at 450 T (green online) in Fig. 3] and F_3 [small peak at 630 T (purple online) in Fig. 3], respectively. The DFT of the fit including all of the Fourier components successfully reproduce these features, as shown in the inset of Fig. 3(a) which displays a zoom of the DFT of the data (symbols) and of the fit (black line) for $\text{YBa}_2\text{Cu}_3\text{O}_{6.54}$. The highest frequency detected in both measurements is F_4 . The field dependence of the main peak of the DFT and of the oscillation amplitude (“Dingle plot”) is displayed in the inset of Fig. 3(b). DFT of the data (symbols) and DFT of the fit (solid lines) are in very good agreement. The black lines show the behavior expected if only one frequency was involved. The strongly nonmonotonic field dependence of

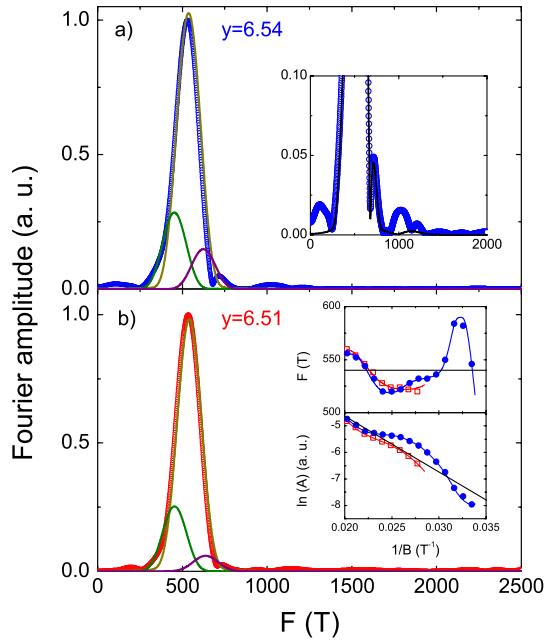


FIG. 3 (color online). Fourier analysis of the oscillatory torque (see Fig. 1) for (a) $\text{YBa}_2\text{Cu}_3\text{O}_{6.54}$ and (b) $\text{YBa}_2\text{Cu}_3\text{O}_{6.51}$ in the field range 31.4–57.4 T. Solid lines show the contribution of F_1 (yellow), F_2 (green), and F_3 (purple), respectively. The top inset shows a zoom of the DFT of the data (symbols) and of the fit including four frequencies (black line). The bottom inset shows the field dependence of the main peak of the DFT and of the oscillation amplitude. Symbols and lines correspond to DFT of the data and DFT of the fit including four frequencies, respectively.

the frequency of the main peak and the apparent non-LK behavior of its amplitude are a signature of several Fourier components with frequencies in a narrow range.

Let us now discuss scenarios which may provide an explanation for the beating effect observed in QO measurements. While it cannot be ruled out that additional FS pockets account for the observed oscillatory spectra, the most natural interpretation is to invoke both a slight modulation of the FS sheet along the c axis (warping) and a bilayer splitting effect, the latter being intrinsic to $\text{YBa}_2\text{Cu}_3\text{O}_y$ which contains two closely spaced CuO_2 planes (separated by 3.2 Å). The bilayer splitting arises from bonding-antibonding coupling of interplane wave functions and gives rise to two CuO_2 plane-derived FS pockets [6]. In band structure calculations for ortho-II- $\text{YBa}_2\text{Cu}_3\text{O}_{6.5}$ in Ref. [23], the warping and bilayer effects led naturally to four frequencies: two come from the bilayer effect and each of them is further split due to warping of the FS (providing that c axis modulation leads to two different extremal areas). Assuming that F_4 is a second harmonic of F_1 (but we cannot rule out that F_4 is a second frequency with a small amplitude corresponding to the hole pocket in a commensurate FS reconstruction [17]), the observation of three frequencies, rather than the expected $4e\hbar$, can be explained either if two frequencies are too close to be resolved or if the amplitude of one frequency is too weak.

There are two hopping terms to consider: t_{\perp}^c comes from the hopping through layers in between the CuO_2 planes and t_{\perp}^b represents the hopping between the planes of the bilayer. In order to estimate t_{\perp}^c , which causes warping of the FS along the c axis, we follow the calculation by Yamaji [24] and assume the simplest form for warping. The quasi-2D dispersion can be written as $\epsilon = \hbar^2/2m^*(k_x^2 + k_y^2) - 2t_{\perp}^c \cos(ck_z)$, where c is the c axis lattice parameter. The c axis warping leads to two extremal FS areas perpendicular to the magnetic field and therefore to two close frequencies that yield a beating effect. From geometrical considerations, the frequency difference is given by $\Delta F = 4m^*t_{\perp}^c/e\hbar$. Assuming that $\Delta F = 90$ T ($F_1 - F_2$ or $F_3 - F_1$), the c axis hopping term $t_{\perp}^c \approx 1.3$ meV, i.e., 15 K. This value is similar to that deduced from the beating effect induced by the warping of the quasi-2D β FS sheet in the quasi-2D oxide Sr_2RuO_4 [25].

In order to deduce a value for the bilayer hopping term t_{\perp}^b , it is necessary to rely on band structure calculations. A model which assumes a reconstruction of the FS can account for the splitting of the frequency linked to the electron pocket frequency into two frequencies $F = 570$ T and $F = 450$ T by considering a bilayer coupling $t_{\perp}^b = 8$ meV [26]. For the unreconstructed FS, band structure calculations predict that $t_{\perp}^b \approx 200$ meV [6,23]. This striking difference in the value of t_{\perp}^b is another indication of the reconstruction of the large hole FS [27].

If warping and bilayer effects are responsible for the observation of several frequencies in underdoped

YBa₂Cu₃O_{6.5}, it thus implies that quasiparticle motion is coherent along the *c* axis at low temperature. While a coherent 3D FS has been established by AMRO experiments in overdoped Tl-2201 [3], a crossover in the phase diagram between a coherent metal phase (overdoped) and an incoherent one (underdoped) has been suggested in Bi₂Sr₂CaCu₂O_{8+δ} [29]. Indeed, both electrical [30,31] and optical measurements [32–34] show that in-plane response can be metallic whereas the out-of-plane response is insulatinglike. The present measurements show that at sufficiently low temperature, when superconductivity is suppressed by a strong magnetic field, the coherence along the *c* axis is restored in underdoped and clean material; i.e., it establishes the existence of a coherent 3D FS, concomitant with the observation of QO.

We end by discussing some open questions raised by the QO in underdoped YBCO. The first is the apparent contradiction with ARPES, which shows the destruction of the Fermi surface in the antinodal regions, producing a set of disconnected Fermi arcs [35,36]. Assuming that ARPES detects only one side of a hole pocket at $(\pi/2, \pi/2)$ [18,37,38] is not sufficient to explain any reconstruction scenario. Indeed, there is no evidence so far in ARPES data of other pockets or regions of the FS where coherent quasiparticles exist, except around $(\pi/2, \pi/2)$. In a stripe scenario [19], the FS contains quasi-1D holelike Fermi surfaces, for which there is no evidence in ARPES data. One proposed scenario to reconcile ARPES and QO measurements is a field induced state [20,21], as suggested by a recent neutron scattering experiment [39]. The second open question concerns the larger frequency ($F_\beta \approx 1650$ T), which has been detected with a very small amplitude in underdoped YBCO ortho-II [11]. The observation of this frequency led the authors of Ref. [11] to suggest a FS reconstruction of the large hole FS into several pockets with different mobilities. In the present study, we were not able to detect this high frequency within a noise level lower than 0.5% of the amplitude of F_1 , while the amplitude of this high frequency (F_β) is reported to be 3% of the main frequency (F_1) in Ref. [11]. Further experiments on different samples should help clarify this apparent contradiction.

In summary, we have achieved very high precision in the measurements of the de Haas–van Alphen effect in underdoped YBa₂Cu₃O_{6.5}. We found no evidence of a larger pocket as claimed in Ref. [11]. A fitting procedure based on the Lifshitz-Kosevich theory has revealed that the main oscillation is in fact composed of at least three closely spaced frequencies, which we attribute to bilayer splitting and warping of the FS along the *c* axis. This interpretation implies that quasiparticle transport perpendicular to the CuO₂ planes is coherent in the underdoped regime at low temperature.

We thank A. Carrington, S. Chakravarty, N. Hussey, M. Norman, G. Rikken, S. E. Sebastian, B. Vignolle, and J. Zaanen for useful discussions. We acknowledge support

from EuroMAGNET under EC Contract No. 506239, the ANR projects ICENET and DELICE, the Canadian Institute for Advanced Research, and funding from NSERC, FQRNT, EPSRC, and a Canada Research Chair.

*proust@lncmp.org

- [1] N. Doiron-Leyraud *et al.*, Nature (London) **447**, 565 (2007).
- [2] B. Vignolle *et al.*, Nature (London) **455**, 952 (2008).
- [3] N. E. Hussey *et al.*, Nature (London) **425**, 814 (2003).
- [4] M. Platié *et al.*, Phys. Rev. Lett. **95**, 077001 (2005).
- [5] A. P. Mackenzie *et al.*, Phys. Rev. B **53**, 5848 (1996).
- [6] O. K. Andersen *et al.*, J. Phys. Chem. Solids **56**, 1573 (1995).
- [7] D. J. Singh and W. E. Pickett, Physica (Amsterdam) **203C**, 193 (1992).
- [8] A. Bangura *et al.*, Phys. Rev. Lett. **100**, 047004 (2008).
- [9] E. A. Yelland *et al.*, Phys. Rev. Lett. **100**, 047003 (2008).
- [10] C. Jaudet *et al.*, Phys. Rev. Lett. **100**, 187005 (2008).
- [11] S. E. Sebastian, N. Harrison, E. Palm, T. P. Murphy, C. H. Mielke, R. Liang, D. A. Bonn, W. N. Hardy, and G. G. Lonzarich, Nature (London) **454**, 200 (2008).
- [12] D. Shoenberg, *Magnetic Oscillations in Metals* (Cambridge University Press, Cambridge, 1984).
- [13] S. Chakravarty, Science **319**, 735 (2008).
- [14] C. Jaudet *et al.*, Physica (Amsterdam) **404B**, 354 (2009).
- [15] L. Taillefer, J. Phys. Condens. Matter **21**, 164212 (2009).
- [16] D. LeBoeuf *et al.*, Nature (London) **450**, 533 (2007).
- [17] S. Chakravarty and H.-Y. Kee, Proc. Natl. Acad. Sci. U.S.A. **105**, 8835 (2008).
- [18] N. Harrison *et al.*, Phys. Rev. Lett. **99**, 206406 (2007).
- [19] A. J. Millis and M. Norman, Phys. Rev. B **76**, 220503(R) (2007).
- [20] W.-Q. Chen *et al.*, Europhys. Lett. **82**, 17 004 (2008).
- [21] S. Sachdev, arXiv:0907.0008.
- [22] R. Liang *et al.*, Physica (Amsterdam) **336C**, 57 (2000).
- [23] A. Carrington and E. A. Yelland, Phys. Rev. B **76**, 140508 (R) (2007).
- [24] K. Yamaji, J. Phys. Soc. Jpn. **58**, 1520 (1989).
- [25] A. P. Mackenzie and Y. Maeno, Rev. Mod. Phys. **75**, 657 (2003).
- [26] I. Dimov *et al.*, Phys. Rev. B **78**, 134529 (2008).
- [27] Note that in YBa₂Cu₄O₈, the same order of discrepancy has been deduced from magnetotransport measurements for the interchain coupling, which has been interpreted as virtual hopping process [28].
- [28] N. E. Hussey *et al.*, Phys. Rev. Lett. **80**, 2909 (1998).
- [29] A. Kaminski *et al.*, Phys. Rev. Lett. **90**, 207003 (2003).
- [30] K. Takenaka *et al.*, Phys. Rev. B **50**, 6534 (1994).
- [31] Y. Ando *et al.*, Phys. Rev. Lett. **77**, 2065 (1996).
- [32] K. Tamasaku *et al.*, Phys. Rev. Lett. **69**, 1455 (1992).
- [33] D. N. Basov *et al.*, Science **283**, 49 (1999).
- [34] C. C. Homes *et al.*, Phys. Rev. B **71**, 184515 (2005).
- [35] M. R. Norman *et al.*, Nature (London) **392**, 157 (1998).
- [36] M. A. Hossain *et al.*, Nature Phys. **4**, 527 (2008).
- [37] S. Chakravarty *et al.*, Phys. Rev. B **68**, 100504(R) (2003).
- [38] J. Meng *et al.*, arXiv:0906.2682.
- [39] D. Haug *et al.*, Phys. Rev. Lett. **103**, 017001 (2009).